Agricultural and Forest Meteorology 264 (2019) 92–103

Contents lists available at ScienceDirect

Agricultural and Forest Meteorology

journal homepage: www.elsevier.com/locate/agrformet

Identifying wildfire-prone atmospheric circulation weather types on mainland Spain

Marcos Rodrigues[a,c,*], José Carlos González-Hidalgo[b,c], Dhais Peña-Angulo[b,c], Adrián Jiménez-Ruano[b,c]

[a] Department of Agriculture and Forest Engineering, University of Lleida, Lleida, Spain
[b] Department of Geography and Land Management, University of Zaragoza, Zaragoza, Spain
[c] Institute University of Research in Environmental Sciences (IUCA), University of Zaragoza, Zaragoza, Spain

ARTICLE INFO

Keywords:
Wildfire
Weather type
Fire season
Synoptic circulation
Pyrogeography
Cluster analysis

ABSTRACT

In this paper we present a detailed spatial assessment of the association between atmospheric synoptic conditions (the weather types, WT) and fires on the Spanish mainland. The WT approach allows the continuum of atmospheric fields to be compressed into a few comprehensive patterns, providing meaningful information on the movement of air masses, wind direction and, ultimately, wind speed. We analyzed a total of 291,547 individual fires from the official Spanish Fire database (1974–2014) and corresponding daily WT patterns on the Iberian Peninsula from the daily NCEP/NCAR Reanalysis database, 1951–2015. Underlying spatial patterns of association among fire and weather types were explored by means of self-organizing maps (SOM) coupled to hierarchical clustering.

Our analyses have detected that fires tend to occur and become largermore likely under certain atmospheric conditions suggesting that specific weather patterns can promote or boost fire events. From a pyrogeographical point of view, the contribution of WTs to wildfires on the Spanish mainland seems to be highly diverse, and displays several temporal and spatial patterns. The northwest region responds mostly to eastern flows during summer and southern during winter. Fires in the northern Mediterranean coast are promoted by northerly flows while in southern regions fires are linked to C or SE extreme heat episodes during summer. Overall, fires activity usually increases in the lee ward of mountain ranges depending on the prevalent flow from WTs, and thus related to adiabatic heating of the air flow.

1. Introduction

Wildfires are recognized as one of the major and recurrent hazards in Mediterranean environments, with a wide range of impacts on humans and ecosystems (San Miguel-Ayanz et al., 2013), as a result of a complex human–environment interaction (Koutsias et al., 2012; Krebs et al., 2010; Liu et al., 2012; Liu and Wimberly, 2015). Nevertheless, it is commonly accepted that over 90% of wildfires are man-made due to agricultural practices, negligence or premeditated actions (Leone et al., 2003; Martínez et al., 2009; San-Miguel Ayanz and Camia, 2009).

The total area affected during wildfires depends on the topography and fuel, among other factors (Papadopoulos et al., 2013), with weather conditions widely accepted to be a crucial factor during initial fire ignition and propagation stages (Thompson et al., 2011; Benson et al., 2008; Ruffault et al., 2017b; Russo et al., 2017).

According to pyrogeography – the study of the spatial distribution of fire across space – favorable weather and climate situations control fire conditions (Meyn et al., 2007; Parisien and Moritz, 2009). In this respect, understanding the relative influence of weather on fire incidence, as well as its potential underlying patterns, may lead to improving fire management strategies. Thus, larger fires have been detected under high temperatures and dry conditions in southern Europe (Camiá and Amatulli, 2009; Urbieta et al., 2015), the Iberian Peninsula (Trigo et al., 2016) and Spanish mainland (Piñol et al., 1998; Turco et al., 2013), where an increased contribution from climate factors on fire ignition was reported by Rodrigues et al. (2016). Weather also controls how fires behave: high temperatures and low humidity dry out fuels to speed up burning (Cardil et al., 2014); wind moves wildfires across landscapes, while also supplying oxygen (Salis et al., 2016); finally, rain and high humidity can slow or even extinguish fires, whereas storms can cause fire activity to increase or become completely unpredictable.

The atmospheric conditions are represented in the atmospheric

* Corresponding author at: Alcalde Rovira Roure 191, 25198, Lleida, Spain.
E-mail address: rmarcos@eagrof.udl.cat (M. Rodrigues).

https://doi.org/10.1016/j.agrformet.2018.10.005
Received 28 April 2018; Received in revised form 5 October 2018; Accepted 8 October 2018
Available online 15 October 2018

synoptic chart (the well-known Weather Chart) which summarizes the continuum of atmospheric pressure fields from which stability or instability and main flow direction can be deduced. This document has been used to produce the Weather Type (WT) classification that aims to categorize the perhaps infinite situations of atmospheric synoptic conditions, represented by the daily weather chart, into fewer and a more manageable number of classes (Trigo and DaCamara, 2000). Following this argument, WTs have been associated with different processes in many research areas, including their relationship with precipitation (Cortesi et al., 2014; Fernández-González et al., 2012; Hidalgo-Muñoz et al., 2011), temperature (Peña-Angulo et al., 2016), air quality (Collaud Coen et al., 2011), atmospheric pollution and human health (Liao et al., 2017; Royé et al., 2016; Santurtún et al., 2015). They have also been used to analyze geomorphological processes (Foster and Lees, 1999; Nadal-Romero et al., 2015; Wilby et al., 1998), run-off (Fernández-Raga et al., 2010), and a variety of natural hazards (Messeri et al., 2016; Teale et al., 2017). Finally, the relationship among WTs and fire activity has been previously studied in certain European regions, such as the Alps (Wastl et al., 2013), the Eastern-Mediterranean (Paschalidou and Kassomenos, 2016), France (Ruffault et al., 2017a, 2017b) and the Iberian Peninsula (Trigo et al., 2016). In the Mediterranean basin, synoptic high pressure conditions were linked to winter fires (Paschalidou and Kassomenos, 2016), while cyclonic conditions were thought to trigger summer events (Ruffault et al., 2017b). However, the majority of these analyses focused on the relationship between weather and burned area, disregarding their role in fire ignition or seasonal differences; a recent exception is the paper by Duane and Brotons (2018) who describe the effect of southerly patterns on large fires.

From an environmental point of view, fires are one of the most important challenges on the Spanish mainland, where gross climate division is the result of its latitudinal position between two contrasting water masses (the Atlantic Ocean and the Mediterranean Sea), and the mostly west to east spatial distribution of mountain ranges (Cortesi et al., 2014; Peña-Angulo et al., 2016) (Fig. 1). These factors, coupled with different air masses during the year, explain the spatial gradients of temperature and precipitation (Martín-Vide and Olcina, 2001) that may cause the spatial differences in fire-prone weather conditions (Montserrat, 2000). Therefore, Spain is usually divided into three major climatic areas: (i) the north coastland; (ii) the central-west to south-west regions; and (iii) the eastern Mediterranean coastland. A recent paper by Jiménez-Ruano et al. (2017) reported an increase in fire activity in the north-western area of Spain, which is one of the most fire-affected regions in Europe (Koutsias et al., 2016). Furthermore, winter fire frequency and large fires have been increasing in Spain since 1974, partially induced by human activities (Moreno et al., 2014), but also related to climate factors (Cardil et al., 2014, 2013; Duane and Brotons, 2018; Rodrigues et al., 2018).

In this research, we present a spatial analysis of the association between atmospheric synoptic weather conditions (the weather type, WT) and wildfires on the Spanish mainland. The paper especially addresses the influence of short-term WTs on fire occurrence and burned area, and the seasonal dissimilarities between winter and summer. In particular, we have analyzed the relationship among fires and WTs from the Spanish Fire Database (1974–2014) and the Weather Types (WTs) estimated from the NCEP/NCAR Reanalysis data. Our main goals were (1) to identify the main atmospheric synoptic patterns expressed by WTs associated with fire, both in terms of occurrence (number) and burned area, (2) to find any differences between winter and summer fires consistent with WTs, and (3) to detect spatially homogenous zones of fire WTs (e.g., WTs associated with fire incidence).

2. Materials and methods

2.1. Study area

The study area encompasses the whole of mainland Spain (Fig. 1). From a climatic perspective, this area is characterized by contrasting climatic conditions from *Cf* oceanic humid conditions in the north-west to Mediterranean *Cs* and steppe *BS* types in the center, south and east. Botanical and biogeographical studies divide Spain into two main areas: the Eurosiberian region, located in the northwest, and the Mediterranean region, covering the remainder. The Eurosiberian area is mostly covered by deciduous and evergreen oak and ash woodlands (*Quercus robur*, *Fraxinus excelsior* and *Fagus sylvatica*); forest plantations of *Pinus radiate* and *Eucalyptus globulus* cover large areas. On the other hand, the Mediterranean region displays complex mosaics of agricultural systems and plant communities. Sclerophyllous and evergreen vegetation, such *as Quercus ilex*, *Quercus suber* and thermophilous scrublands dominate the region, whereas forest systems mainly consist of pine species (*Pinus halepensis*, *Pinus sylvestris*, *Pinus nigra*, *Pinus pinea* or *pinaster*), see Fig. 1.

2.2. Weather type classification

Historically, the WT approach includes subjective classifications based on the opinions of experts (e.g. Lamb, 1972), and others based on

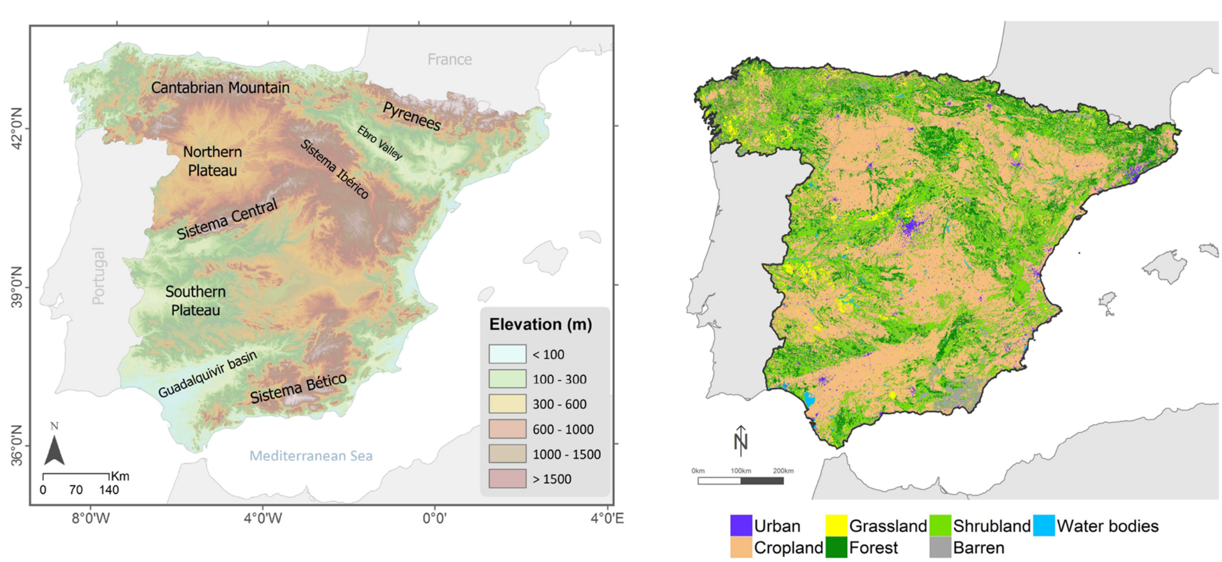

Fig. 1. Study region. Left, relief and main mountain ranges; right, spatial distribution of main cover types according to Corine Land Cover 2000.

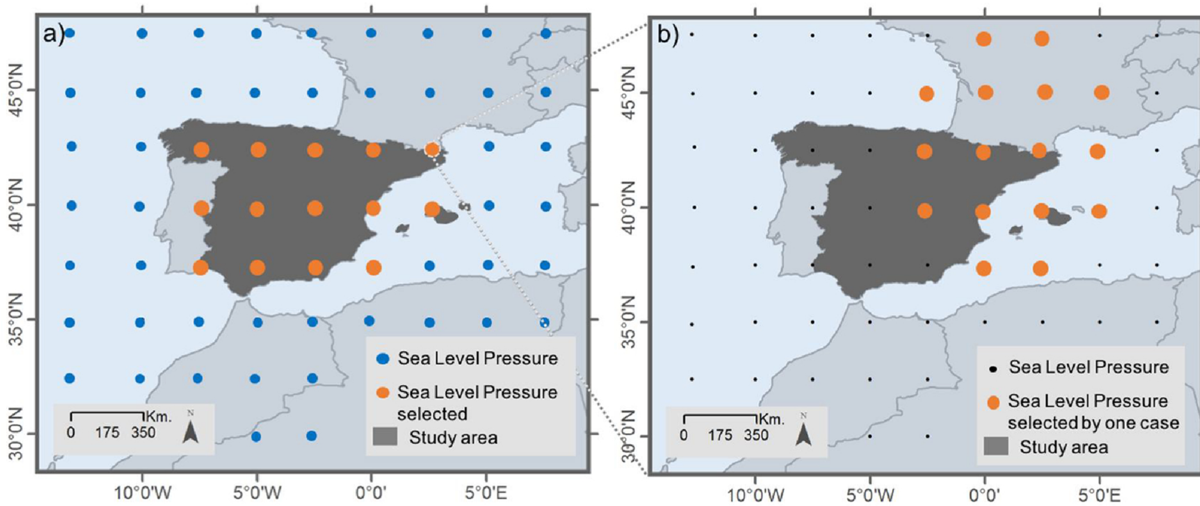

Fig. 2. Left, location of SLP nodes in the NCEP/NCAR Reanalysis; right, an example of node selection from the database to calculate WT in northeast of Spain.

automatized techniques (Yarnal et al., 2001; Huth et al., 2008; Phillip et al., 2010). Amongst these, the subjective one proposed by Lamb (1972) for the British Islands, adapted to an objective algorithm by Jenkinson and Collison (1977), improved later by Jones et al. (1993), and adapted to the Iberian Peninsula by Trigo and DaCamara (2000), is one of the most widely used, because of its feasibility. In the classification identifying the daily circulation weather types, the direction and strength of airflow, and cyclonic conditions from sea level pressure grid are calculated.

The normalized procedure of daily classification includes a set of 15 total pressure values around the target ones (16 sea level total pressure values, see Fig. 2), in which the following indices are calculated: southerly flow (FS), westerly flow (FW), total flow (F), southerly shear vorticity (ZS), westerly shear vorticity (ZW) and total shear vorticity (Z). The six indices, formulae and rules can be found in Trigo and Da Camara (2000) and they enable 26 different circulation WTs to be defined on a daily scale, usually grouped into three main classes: eight pure directional types defined by their compass direction, two pure types controlled by the strength of geostrophic vorticity (anticyclonic A, cyclonic C), and sixteen hybrid types that combine the previous ones (see Trigo and Da Camara, 2000; Cortesi et al., 2014). The classification has been broadly used for studying climate variability in the Iberian region and has shown the high capability of WT to identify spatial and temporal relationships with temperature and precipitation (Cortesi et al., 2014; Peña-Angulo et al., 2016). At the root of this relationship, it must be understood that WTs provide information on the main direction of air masses, i.e. where the air comes from.

The method was applied to daily pressure data of the 14 nodes covering the Spanish mainland and Balearic Islands from the grid points of the NCEP/NCAR Reanalysis database (1951–2015); grid nodes were spaced across latitude 2.5° and longitude 2.5° (Fig. 2). The 26 WTs obtained on a daily basis were recoded according to the directional component to obtain a final set of 10 WTs (N, NE, E, SE, S, SW, W, NW and pure A and pure C). This reclassification was due to simplifying the original 26 classifications into a more manageable number, and because we were mostly interested in the provenance of the air mass rather than its specific barometric properties. For detailed analyses of reclassification and procedures for analyses on the Iberian Peninsula, see Cortesi et al. (2014) and Peña-Angulo et al. (2016).

2.3. Fire data

Fire data was provided by the Ministry of Agriculture, Food, and Environment, compiled by the Forest Fire Department. Database reports include information on the starting point of fire (recorded on a 10 x 10 km reference grid), total burned area, ignition source, etc. The period from 1974 to 2014 was analyzed, as prior to this, fire events had only been recorded at province level and thus information was not available at grid scale. A total of 291,547 events were analyzed with information retrieved for each one on the detection date (to match with WT), initial grid point location, and total burned area. We discarded small fires (less than 1 Ha burned) or those with insufficient data (location or size).

Fig. 3 shows the spatial distribution of total fires and surface burnt in the long summer (May to September) and long winter (October to April) seasons. Irrespective of the season, there are areas in which a high number of fires were found, and the total land burnt reached 2,000 ha, although with apparent differences between the long seasons of winter and summer.

2.4. Analyses

We approached the fire-WT relationship in three steps: (1) first, by analyzing the spatial frequency distribution of fire under different WTs; (2) next by investigating the relationship among WTs and burned area; (3), finally, by attempting to identify spatial aggregation of fire activity according to WT. All the analyses were carried out by dividing fire data into long summer and long winter seasons, given the well-known intra-annual distribution of fire frequency and burned area in the Iberian Peninsula. Data analyses were performed at global scales in steps 1 and 2, and from the grid cell fire database, i.e. at local scale.

All statistical procedures, maps and plots used the R statistical programming language (R Core Team and R Development Team Core, 2017), packages *nortest* for normality tests; *dunn.test* for multiple comparison; *rgeos, raster* and *rgdal* for spatial data manipulation; *kohonen, nbClust* and *factoextra* for cluster analysis; and *ggplot2* for mapping and plotting.

2.4.1. Fire frequency and WTs

Each single fire event was added to its corresponding grid cell and assigned to the closest WT node (see Fig. 2). They were then classified according to the WT observed on their respective ignition dates.

The WTs do not occur equally across time, with certain WTs being more frequent than others. Therefore, we hypothesized that, if fire occurrence was random, the observed frequency of fires for each WT must follow the same distribution as that from expected WTs; otherwise, we could infer that the frequency of fires would tend to occur during specific WTs. To test the independence of the frequency of fires and WT, we applied the χ^2 test comparing the frequency distribution of fires according to WTs, and the frequency distribution of WTs at annual scale.

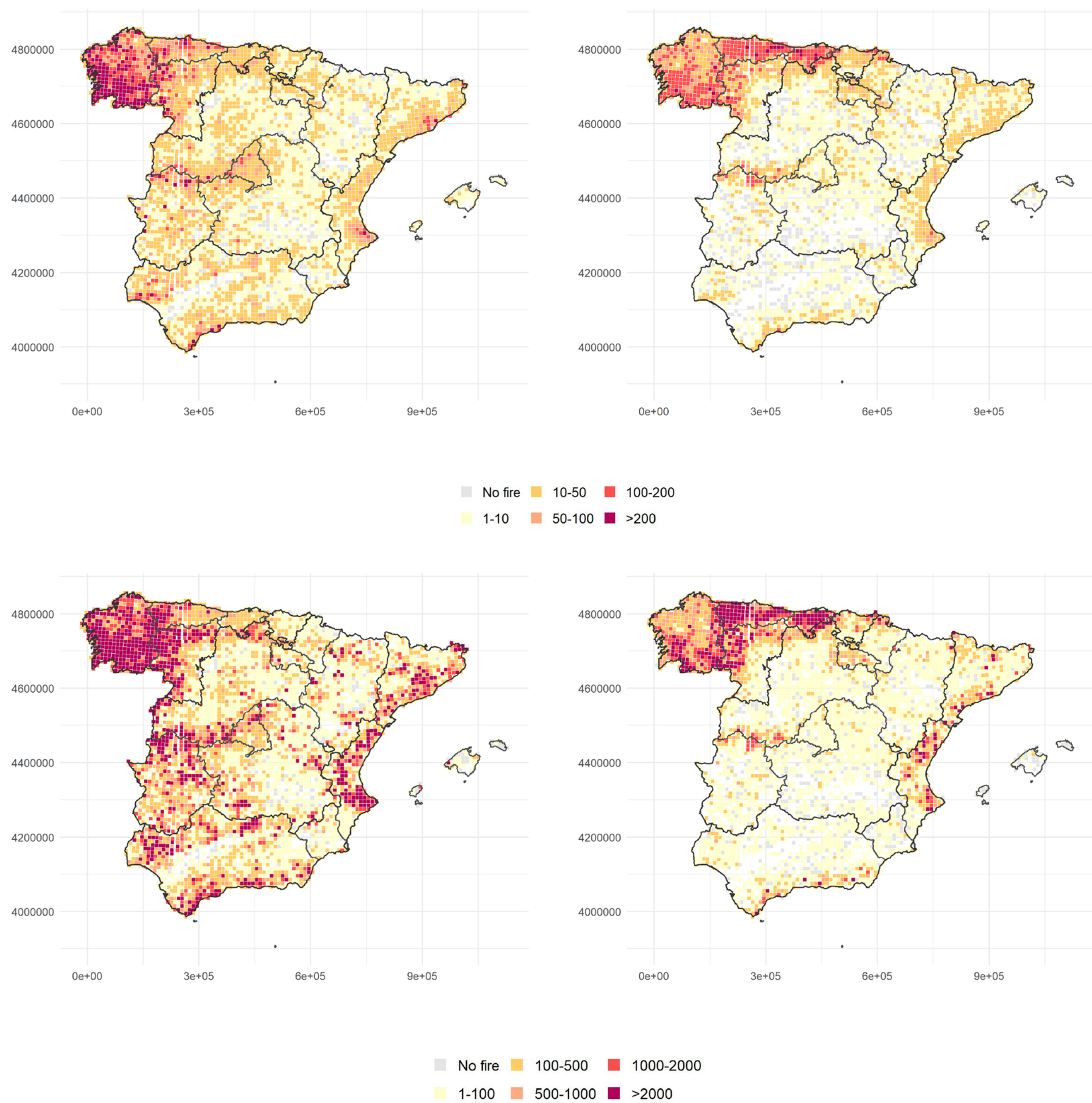

Fig. 3. Spatial distribution of fire activity 1974–2014 at fire grid level. Top, number of fires; bottom burned area (Ha); left, summer fires; right winter fires.

2.4.2. *Total burned area and WTs*

The second step of our analyses was to detect whether WTs influenced the size of the fires, i.e.: if specific WTs promoted larger fires. In this case, because of non-normality of data, we applied the multiple comparison test with unequal sample sizes by Kruskal and Wallis (Kruskal and Wallis, 1952; Wheater and Cook, 2000) and a posteriori Dunn´s test (Dunn, 1964), under the $H_1 > H_0$ hypothesis, i.e.:whether there is a statistical significance in fire size (being larger) under a specific WT than the area burned under other WT conditions.

2.4.3. *Spatial aggregations of WTs*

The objective of the spatial aggregation analysis is to group fire grid cells (Fig. 3) into clusters of WTs so that fires within one cluster share more in common with each another than they do with the fires in other clusters. The analysis of spatial aggregations of WTs was performed with Self Organizing Maps (SOM) combined with hierarchical clustering on fire data to WT and fire grid cell. To reduce the amount of inputs, we selected cells with more than 5 summer fires (87.8% of fires), and 5 winter fires (86.0% of fires), with 112 ha burned in summer (97.7%) and 54 ha burned in winter (96.9%). These thresholds are all in the 3rd quartile of the overall distribution of fire frequencies and burned area per season.

The SOM (20 × 20 SOM-grid, 10,000 iterations and learning rates from 0.1 to 0.0001) and hierarchical clustering were used to build the final clusters per fire feature and season. SOM enabled pre-classification of fires over a 2-dimensional 20 × 20 SOM-grid, so that each fire was allocated in a node. Next, hierarchical clustering was applied to SOM grid nodes. We retrieved 4 sets of clusters (summer/winter ignitions and burned area). Several parameterizations were explored before eventually selecting the Euclidean distance and *ward.D2* agglomeration criterion (Sorensen, 1948) for fire frequency, and *canberra* and *complete* for the burned area. A key step towards a successful cluster analysis is to determine the amount of clusters. We optimized the proposed clustering strategy using the *nbClust* R package using all indexes according to the highest ranked number of clusters. The *nbClust* implements 30 indices based on different criteria, a brief description of which can be found in (Charrad et al., 2014), along with further references to each index.

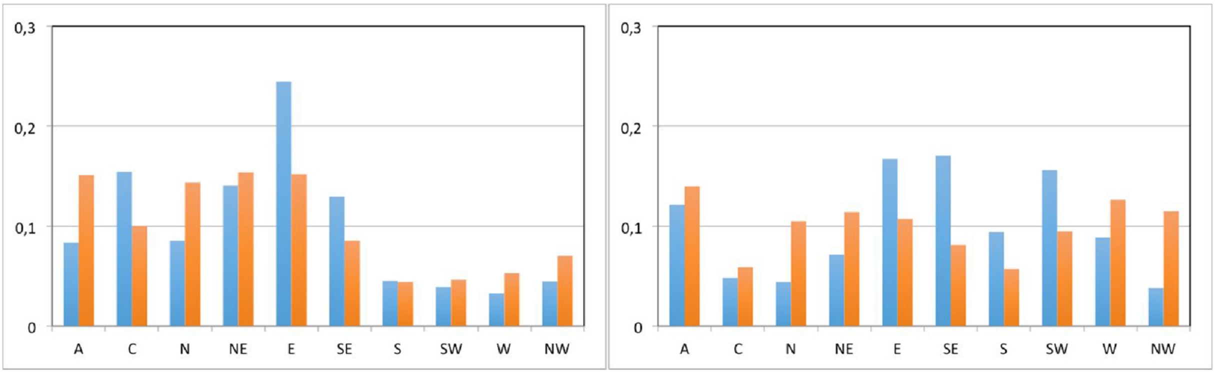

Fig. 4. Summer (left) and winter (right) frequency distribution of fires by WT (blue) and total WT frequency daily distribution (orange). Data rounded (For interpretation of the references to colour in this figure legend, the reader is referred to the web version of this article.).

3. Results

3.1. Fire frequency and WTs

The total observed distribution of fires per WT and the frequency distribution of WTs are presented in Fig. 4 for summer and winter. According to the χ^2 test, the distribution of fire occurrence per WT differs significantly from the WTs observed in both seasons ($p < 0.05$), and consequently, it can be assumed that fires generally tend to occur under specific atmospheric conditions.

During summer, the largest number of fires occurred under E synoptic WT conditions (> 20% of total fires), followed by C, NE, and SE (each with > 10% of total fire). Fire frequency under these WTs was higher than the total frequency, except for NE. These results suggest that in summer, fire frequency tends to accumulate under these synoptic patterns (66,8% of total fires) in particular. In Fig. 5, we show the sea level pressure pattern for C, E, NE and SE weather types. Except for the C type, the Azores high-pressure center plays a major role depending on its position.

Winter displays a different pattern. While, as in summer time, fires tend to concentrate under E synoptic pattern again (although to a lesser extent), fire frequency is also high under SW and SE synoptic conditions (all > 10% of total fires), while the A type emerges. We also noticed that frequency distribution of WTs differ from that of summer time. It is worth highlighting the fact that the relationships between fires and WT in winter are very different from those in summer, and fires are particularly concentrated in southerly WTs such as SE, SW and S. In contrast with summer, fire frequency under C decreases whereas it increases under SW, both in terms of WT frequency and fires triggered under these conditions. Finally, we especially noticed the high fire frequency under A conditions in winter months. Fig. 6 shows the A and SW pattern of sea level pressure.

3.2. Burned area and WTs

General statistical descriptors of summer and winter fires are presented in Table 1. In general, the mean size of summer fires is higher in all WTs (> 20 Ha) than in winter (< 20 Ha, except NW); the highest number of fires was found under E atmospheric conditions, and total burnt area was over 1 million ha under C and E. Meanwhile, in winter the total burnt area never exceeds 350,000 ha and, except under NW conditions, mean values never reach 20 Ha. It is striking that under C

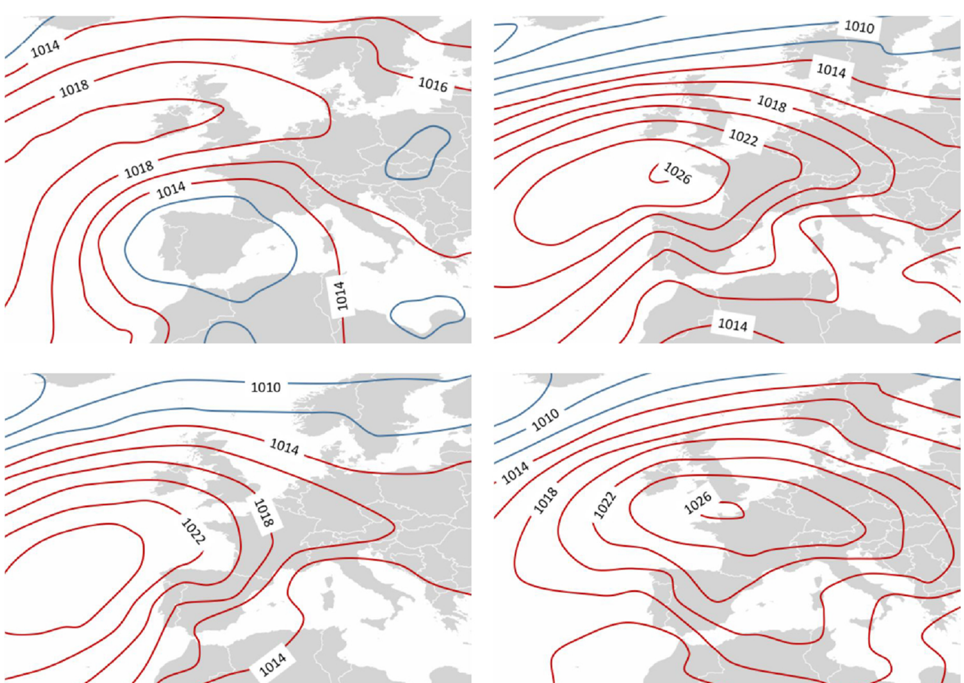

Fig. 5. Sea surface pressure under C and E (top), NE and SE (bottom) Weather Types.

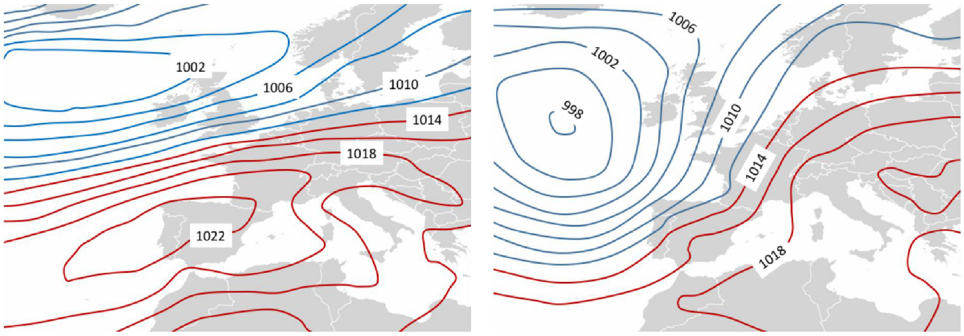

Fig. 6. Sea surface pressure under A and SW Weather Types.

conditions the total burnt area decreases considerably with respect to summer.

The results from the comparison of fire size under different WTs are presented in Tables 2 and 3. Global results suggest that during the long summer season (Table 2), fire size under C and E synoptic conditions is usually significantly higher than those burning under northerly flows (NW, N, NE) and W, but do not greatly differ from fires triggered under southerly flows (SW, S, SE). In addition, total fire size under northerly flows is usually smaller than with southerly flows (SW, S, and SE). It is interesting to note that fire size under an A synoptic WT is significantly smaller than with any WT except NE and W.

Table 3 shows the results of the pairwise comparison for winter. Fire size under southerly (SW, S, SE), and W patterns is normally higher in comparison with other WTs. Unlike summer, the fires under A synoptic conditions are significantly higher than those burned under northerly flows (NW, N, NE) or cyclonic conditions. It is also noticeable that, in winter, fire sizes are much more variable under the different WTs than in summer (see Table 1).

3.3. Spatial aggregation of fire and WTs

Cluster analysis was applied to fire frequency and burned area data in the long summer and long winter, separately.

3.3.1. Fire frequency

The spatial distribution of burned cells during summer can be grouped into 4 clusters that show clearly dissimilar patterns and association with WTs (Table 4). The spatial pattern (Fig. 7) is dominated by Cluster 4, which includes more than 50% of total summer fires (> 90,000 fires), while Clusters 1, 2 and 3 each include less than 20% (< 30,000 fires). The global relationship among WTs and clusters suggests that the most conspicuous synoptic weather patterns in summer are C, followed by E and SE, due to their contribution to each cluster. As a general summary, cluster analyses of summer fire frequency indicate (i) the weak effect of westerly flows on fires (never > 10%), (ii) the global effect of C synoptic WT conditions producing at least 10% of fires in any cluster, and (iii) the generalized effect of easterly flows (NE, E, SE).

Cluster 1 includes 36.1% of the analyzed area (grid cells) and 16.3% of events. The cluster aggregates fires mostly related to SE (34.7%) and C (30.9%) WTs. These fires are mainly located in the mid-southwestern area of Spain along the edges of the Guadalquivir basin and south of the Sistema Central range. The cluster characterizes many sites (cells), although with few fires (16.3%), suggesting that recurrence on the same site is low (Fig. 7). Cluster 2 comprises 11.6% of the area and 8.2% of fires, It is related to mainly easterly patterns (NE, E, SE), with SE and NE causing the most fires; also N, S and C conditions are linked to more than 10% of ignitions; fires were most frequently located in the extreme northeast of Spain and the mid-western areas of the south face of the Sistema Central range (Fig. 7). Cluster 3 is the smallest in terms of area affected (9.9%) and fire counts (10.7%). The events are mostly related to E and, to a lesser extent, SE flows, affecting the coastland areas north of the Cantabrian Mountain range. Also more than 10% of fires arise under C and A patterns. Finally, Cluster 4 represents the most widespread combination of fire frequency during summer (Fig. 7); it includes 42.4% of total area and 53.2% of summer fires. The cluster is characterized by the E synoptic WT conditions (35.7% of fires), followed by NE (18.4%); as with cluster 3, the A and C synoptic WTs cause more than 10% of fires, but not the SE type. The fires are distributed in two highly contrasting areas, but which are both severely affected by fire.: the extreme northwest and along the Mediterranean coast in the east. This cluster features the largest amount of fires. Finally, there are analogies with cluster 3 in respect of WTs, except that the SE changes to NE in cluster 4.

The association between fire ignition and WTs during winter is different from summer, and no generalized WTs emerge from the clusters (Table 5; Fig. 8). Consequently, more WTs seem to be associated to fire ignition in winter than in summer at the local scale. We

Table 1
Summary of fire activity per WT and season (1974–2015). N, number of fires; B. Area, total burned area (ha); Avg. size, average size of fires; and Median size, median size of fires.

	Summer				Winter			
WT	N	B. Area	Avg. size	Median size	N	B. Area	Avg. size	Median size
A	14307	309767	21.6	4.1	14643	150671	10.3	4.0
C	26407	1046731	39.6	5.0	5828	77786	13.3	4.0
E	41810	1040345	24.9	5.0	20142	240110	11.9	4.0
N	14599	383603	26.3	4.4	5323	102285	19.2	3.5
NE	24035	673551	28.0	4.9	8632	101398	11.7	4.0
NW	7665	247644	32.3	4.5	4591	111942	24.4	4.0
S	7760	281687	36.3	5.0	11351	143341	12.6	4.5
SE	22136	692459	31.3	5.0	20531	255648	12.4	5.0
SW	6704	200511	29.9	5.0	18791	308867	16.4	4.1
W	5608	152651	27.2	4.0	10684	124351	11.6	4.2

Table 2
Long summer season, Dunn test pairwise comparison, following the Kruskal-Wallis test, between fire size under different WTs. (*) significance at $p < 0.05$.

	A	C	N	NE	E	SE	S	SW	W
C	−10.09*								
N	−4.83*	4.65*							
NE	−2.94	8.27*	2.45						
E	−11.14*	−0.40	−5.31*	−9.50*					
SE	−9.41*	0.42	−4.13*	−7.50*	0.84				
S	−6.31*	1.22	−2.29	−4.44*	1.53	0.90			
SW	−6.42*	0.70	−2.59	−4.63*	0.97	0.42	−0.36		
W	−0.01	7.11*	3.60*	2.07	7.57*	6.73*	5.06*	5.24*	
NW	−4.41*	3.25*	−0.40	−2.40	3.65*	2.89	1.64	1.94	−3.54*

Table 3
Long winter season, Dunn test pairwise comparison following the Kruskal-Wallis test, among fire size under different WTs. (*) significance at $p < 0.05$.

	A	C	N	NE	E	SE	S	SW	W
C	6.55*								
N	5.15*	−0.99							
NE	15.54*	6.45*	7.36						
E	1.75	−5.54*	−4.12*	−14.91*					
SE	0.23	−6.66*	−5.20*	−16.24*	−1.66				
S	−8.23*	−12.68*	−11.17*	−21.98*	−10.40*	−9.02*			
SW	−21.34*	−22.46*	−20.47*	−34.32*	−25.08*	−23.56*	−11.12*		
W	−5.73*	−10.70*	−9.26*	−19.61*	−7.68*	−6.32*	2.23	13.40*	
NW	6.71*	0.61	1.54	−5.33*	5.78*	6.80*	12.38*	21.19*	10.56*

found a set of 5 clusters of WTs in winter fire frequency. Clusters 1, 2 and 4 include a small number of fires (< 5% each), whereas clusters 3 and 5 account for more than 75% of total fires, even though their spatial distribution is very different and the area affected differs significantly (29.9% and 50.9%).

Cluster 1, characterized by northerly flows (NW, 35.5% and N, 39.1%), and includes fires located along the mid-Mediterranean coastland in the lee of the Iberian Mountain Chain. Cluster 2 is dominated by the NE pattern (74.5% of fires) and to a lesser extent by N (20.4%); fires are found in the extreme northeast from the coast to the inland. Cluster 3 contains 30% of total fires and is related to SW (29.2%) and southerly flows (SE, S), also westerly (W), each having more than 10% of fires. Also, over 10% of events are linked to A patterns. Fires occur especially in the northern coastal areas. Cluster 4 includes a low percentage of fires, even though they appear to be a very specific case, given their location at the foothills of the northern inland plateau, mostly related to easterly flows (NE, E and SE), but predominantly under A conditions (34.1%). Finally, Cluster 5 includes a high percentage of winter fires (41.8%) and is mostly linked to easterly and southerly flows, E, SE and SW (not S with < 10%), and A synoptic conditions. The fires are confined to the extreme northwest of the Iberian Peninsula, and also on the north versant of the Central Mountain range.

3.3.2. Burned area

Summer fire analyses identified 3 different spatial aggregations among burned area and WTs (see Fig. 9 and Table 6).

Generally speaking, the spatial aggregation of burned areas under WTs is more diverse than that observed for fire frequency, because fire spread is more complicated than ignition, with a number of factors involved in the final dimensions of a fire (fuel load, extinguishing methods, etc.). Clusters 1 and 2 include most of the burned land, while Cluster 3 shows a much smaller area (Table 6). It is noticeable that no cluster contains more than 10% of the area burned under A conditions, but the three clusters include more than 10% of burned area under C conditions. Cluster 1 is related to easterly flows (NE, E and SE) and C conditions, and is strongly identified in the extreme northwest and Mediterranean coastland. Cluster 2 occurs mainly under C and E conditions, and to a lesser extent SE and N. Finally, Cluster 3 is linked to several WTs, mostly C and S (Fig. 9).

In the end, five clusters were detected for winter fires, according to the total burnt area (Table 7, Fig. 10).

The most prominent and frequent WTs were E and SE flows, but the cluster differs not only in the overall contribution of WTs, but also in the number of synoptic conditions, which are fewer than in summer time. Cluster 1 is related to E and SE flows (particularly SE) and A conditions. Fires are mostly located in the west of the Iberian Peninsula. Cluster 2 contains the most extensive area (38.2%), mainly relating to the southern flow from E to W conditions. Although SW predominates, atmospheric conditions identifying the cluster are very variable, even though the spatial location of the area is mostly confined to the north and eastern coastland zones (Fig. 10). Cluster 3 is mainly related to westerly flows (SW, W and NW), and also C conditions, with most of the fires again located in the eastern part of the Iberian Peninsula. Cluster 4, on the other hand, is linked to easterly flows (NE, E, SE), also A, with no clear distribution pattern on a spatial level. Finally, Cluster 5 is well-defined in the extreme northwest and some areas of the eastern coastland. It is mostly linked to E and SE flows, but also N conditions (Fig. 10).

Table 4
Cluster analysis for summer fire frequency.

ID	Cells	(%)	Fires	(%)	A	C	N	NE	E	SE	S	SW	W	NW
1	689	36.1	27938	16.3	0.5	30.9	12.0	5.4	8.5	34.7	2.0	0.1	0.1	5.7
2	221	11.6	14041	8.2	1.2	14.6	13.1	20.2	13.8	19.3	15.7	1.7	0.1	0.3
3	189	9.9	18381	10.7	12.2	13.8	3.6	8.6	27.6	11.9	2.5	8.6	8.4	2.9
4	809	42.4	91066	53.2	10.7	13.1	7.4	18.4	35.7	6.7	0.9	2.5	2.1	2.6
Total	1908		151426	88.5										

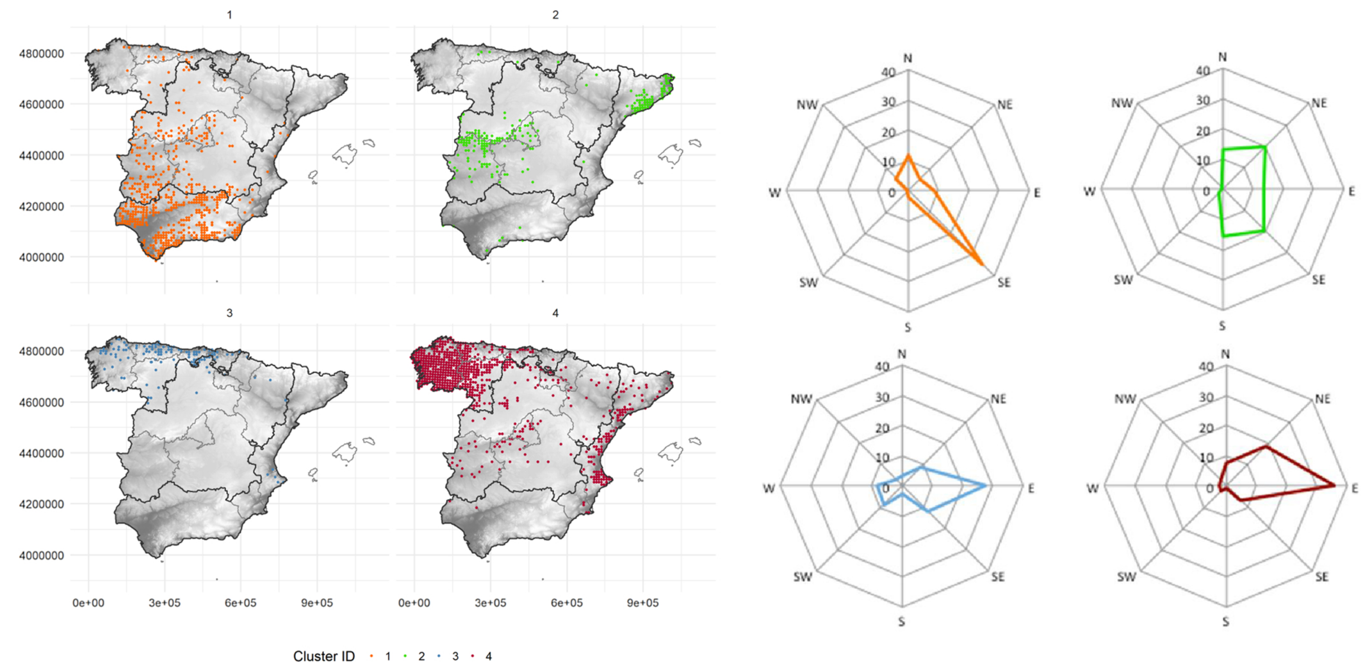

Fig. 7. Spatial distribution of summer clusters of fire frequency (left) and contribution of directional WTs (right).

Table 5
Cluster analyses, winter fire frequency.

ID	Cells	(%)	Fires	(%)	A	C	N	NE	E	SE	S	SW	W	NW
1	132	13.0	4130	3.4	4.2	1.1	39.1	8.5	1.2	4.6	0.0	0.0	5.8	35.5
2	93	9.1	2059	1.7	3.3	0.0	20.4	74.5	0.0	0.0	0.0	0.6	0.0	1.2
3	304	29.9	43615	36.2	11.9	4.1	0.5	1.0	9.8	12.4	12.6	29.2	17.5	1.0
4	103	10.1	5086	4.2	34.1	0.8	4.6	10.0	17.4	14.2	3.7	7.1	4.2	3.9
5	518	50.9	50378	41.8	11.4	4.0	1.6	7.0	27.8	27.0	8.7	10.3	1.8	0.4
Total	1018		105268	87.3										

4. Discussion and conclusions

Fires are one of the main natural and man-made disasters on the Spanish mainland, and the events during the autumn of 2017 were the latest case in which weather conditions of wind coupled with drought caused widespread damage in the northwest, including casualties, extensive burned areas and significant economic loss.

In this research, we have tried to improve the knowledge of fire incidence by studying the atmospheric weather conditions defined by the WTs, using historical fire records from 1974 to 2014. As WTs resume the atmospheric continuum, they provide data on the origin of flows and indirectly suggest information on temperature and humidity conditions. As we stated in previous paragraphs (see introduction section), this approach has been used in former fire research around the Mediterranean basin. Based on this, the present paper gives a detailed analysis of the relationship between atmospheric WT, fire ignition and burned area in Spanish mainland with the aim of finding information valuable to fire management practices, particularly at prevention stages.

Overall, we observed how just a few situations trigger most fires (SE, E, C, SW and A patterns), whereas the burned area is connected to a larger number of WTs. Our findings support the existence of very contrasting summer and winter fire-prone WTs. While eastern flows contribute during the whole year, the influence of the other WTs is often limited to a single season.

The seasonal analysis identifies differences between long summer and winter seasons. Summer fires are triggered in close association with low-pressure systems defined by the C pattern (occasionally thermal lows), and easterly advections (SE and E) promoted by high pressure centers located to the north or northwest of the Iberian Peninsula. Similarly, C and E situations seem to promote the largest fires during the summer season (Table 2). Meanwhile, winter fires seem to be related to a larger number of WTs, with easterly synoptic patterns (such as E, SE) being the most effective in terms of number of ignitions, but also the Atlantic westerly advection. It is noticeable that the A pattern emerges as a highly frequent weather condition under which fire starts. Southerly advections (SW and S) are observed to boost fire size, and are related to larger fires during winter (Table 3). In general terms, both the number of fires and burnt area are lower in any WT in winter than in summer.

The aforementioned associations are not spatially stationary. The cluster analysis enabled a number of spatial configurations to be captured, suggesting that the link between WTs and fires is spatially dependent. The northwest region responds mostly to eastern flows during summer, with a fairly large contribution of SE advections in winter. Westerly advections, such as SW and W, account for the majority of fire activity on the northern face of the Cantabrian Mountains during winter. Fires in the northern Mediterranean coast are promoted by northerly flows (N and NE), whereas the mid-Mediterranean area responds to NE during summer and NW during winter. Fire incidence in southern regions occurs particularly in summer, linked to C and SE extreme heat episodes. This multiplicity of spatial patterns and WTs gives information on the complexity of weather-fire interactions.

One of the most striking results is that fires usually increase in the lee of mountain ranges, depending on the prevalent flow from WTs, and thus should be related to adiabatic heating of the air flow that may enhance fire ignition, because of decreased relative humidity, according to the Clausius-Clapeyron law, thus promoting dry conditions and more

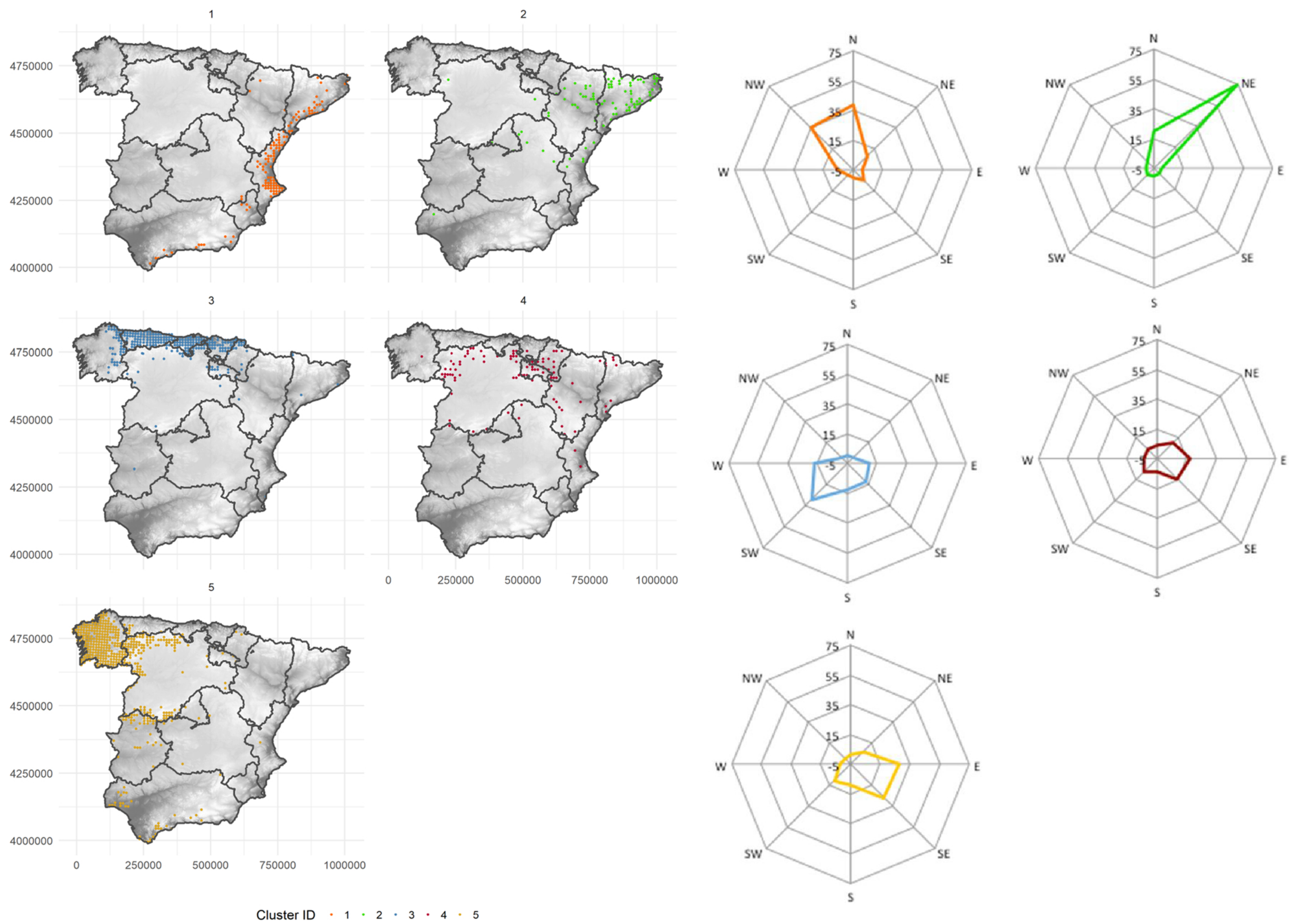

Fig. 8. Spatial distribution of winter clusters of fire frequency (left) and contribution of directional WTs (right).

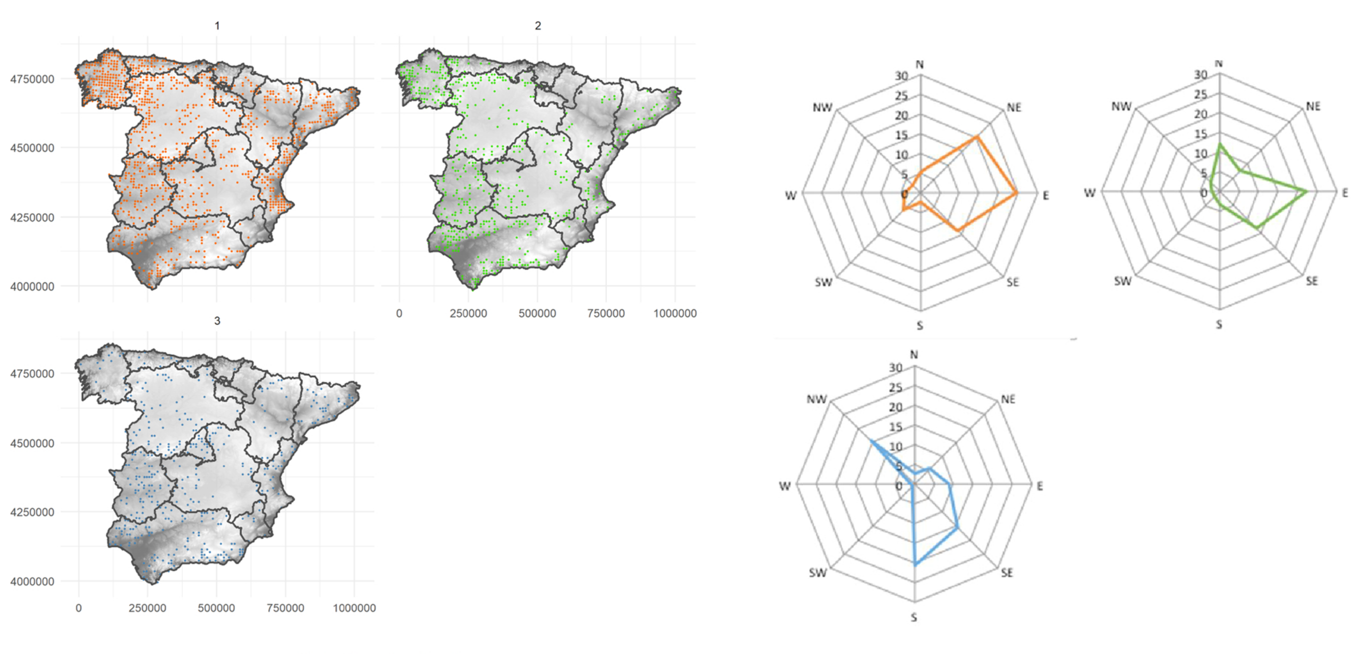

Fig. 9. Spatial distribution of summer clusters of burned area (left) and contribution of directional WTs (right).

Table 6
Cluster analyses, summer burned area.

ID	Cells	(%)	Fires	(%)	A	C	N	NE	E	SE	S	SW	W	NW
1	1189	52.8	2491862	49.6	9.0	12.2	5.4	20.4	24.4	13.5	2.4	5.9	4.0	2.8
2	635	28.2	1736363	34.5	3.5	31.8	12.0	7.4	22.1	13.3	3.3	1.7	1.7	3.1
3	430	19.1	685084	13.6	1.6	27.9	2.8	5.5	9.0	15.6	20.7	0.7	0.7	15.5
Total	2254		4913311	97.7										

Table 7
Cluster analyses, winter burned area.

ID	Cells	(%)	Fires	(%)	A	C	N	NE	E	SE	S	SW	W	NW
1	151	11.1	146573	9.1	11.5	1.1	0.7	1.2	13.6	43.6	4.4	14.2	7.9	1.6
2	353	26.0	618192	38.2	8.1	4.7	2.9	1.7	10.4	12.7	11.1	36.4	10.4	1.5
3	242	17.8	219446	13.6	2.7	10.4	3.6	2.0	2.9	6.0	9.4	14.2	10.8	38.1
4	317	23.3	315640	19.5	18.4	3.0	6.0	13.4	16.4	21.3	6.9	7.6	4.5	2.5
5	296	21.8	265831	16.4	2.6	0.6	17.5	9.2	39.8	15.7	6.6	6.9	0.5	0.6
Total	1359		1565681	96.9										

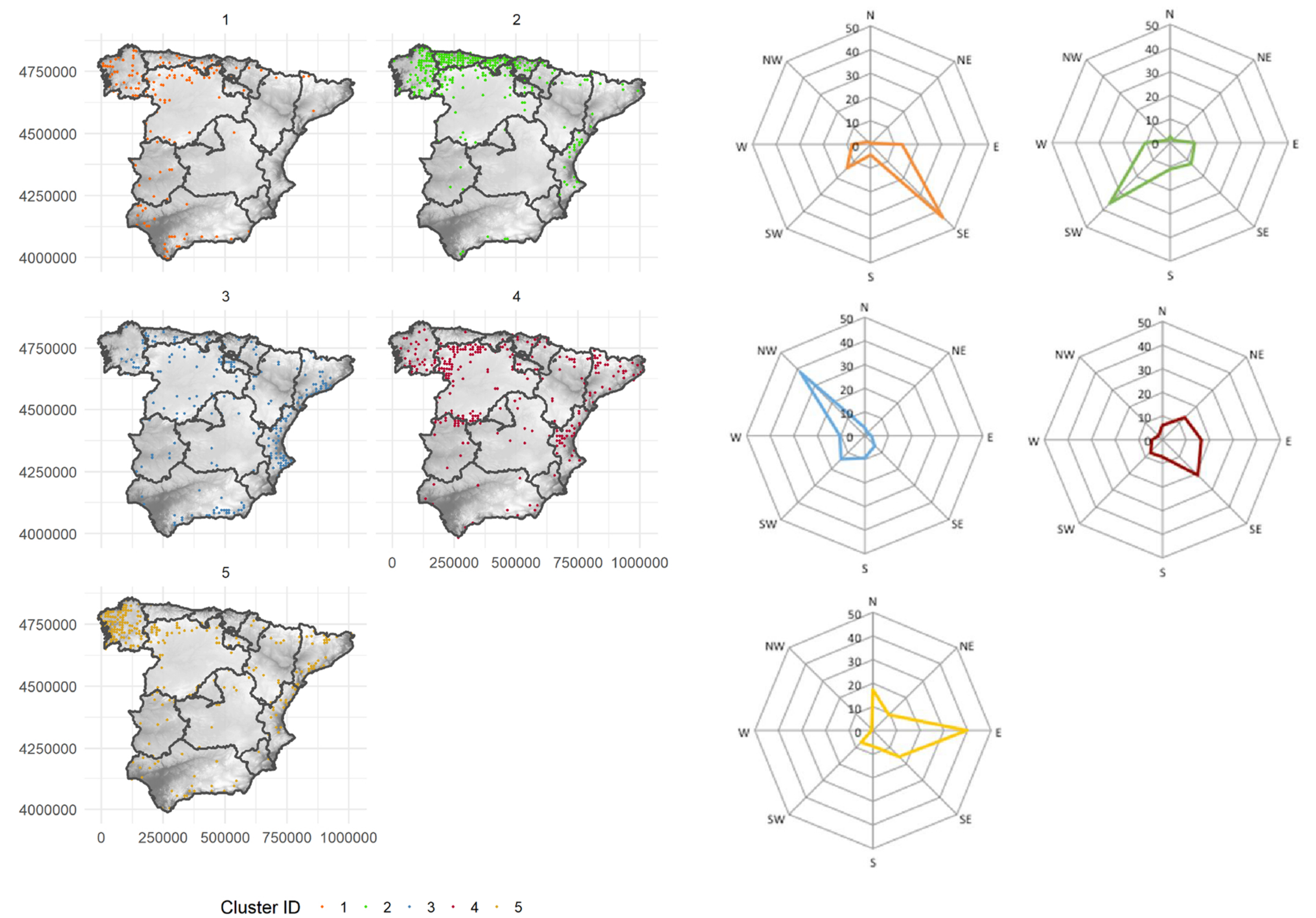

Fig. 10. Spatial distribution of winter clusters of burned area (left) and contribution of directional WTs (right).

hazardous fuels (Holsinger et al., 2016; Salis et al., 2016). This is the case of summer fires on the northern side of the central inland mountain ranges under E and SE flows, the northern coastland under SW and S conditions during winter, and lastly, the eastern coastal areas under NW and W flows. Nevertheless, the spatial pattern identified for forest fires should also be related to other factors, such as the spatial continuum of vegetation cover, its phenology, and the previous weather conditions.

In contrast, we did not detect a clear spatial pattern of WTs in burned area during summer, because the affected area depends on more factors, particularly during the initial stages. Thus, fire events during summer last longer than in winter (MAPAMA, 2012), and, since our analyses only include the synoptic WT on the day of ignition, we are not addressing the full picture. Further research on this topic (i.e. WTs during previous days) should be done. However, similar to fire frequency, eastern advections and cyclonic situations regulate most of the burned area during summer. Again, it is worth mentioning the role of southerly advection, which promotes increased burned areas in the hinterlands and was identified as 'more effective' than A and NE situations in terms of fire size (Table 1). In turn, the spatial distribution of clusters of winter burned areas closely follows the pattern of fire frequency, suggesting that weather conditions during fire ignition control the ultimate size of fires to some extent. This is particularly interesting in the case of the S pattern which, despite being the most uncommon WT (Fig. 4), favors larger fires (Duane and Brotons, 2018).

Acknowledgements

This work is supported by the projects CGL2014-52135-C3-3-R and CGL2017-83866-C3-1-R, financed by the Spanish Government, Ministry of Economy and Finance and FEDER, and the Regional Council of Aragón DGA-FSE (Grupo de Investigación Consolidado 'Clima, Agua, Cambio Global y Sistemas Naturales'). Marcos Rodrigues Mimbrero is a postdoctoral research fellow in the Juan de la Cierva program supported by the Spanish Ministry of Economy and Finance (FJCI-2016-31090); Adrian Jiménez-Ruano is a granted FPU-PhD student (Ref. 13/06618). We also thank the reviewers for their insightful comments which have contributed to improve our work.

Appendix A. Supplementary data

Supplementary material related to this article can be found, in the online version, at doi:https://doi.org/10.1016/j.agrformet.2018.10.005.

References

Benson, R.P., Roads, J.O., Weise, D.R., 2008. Chapter 2 Climatic and weather factors affecting fire occurrence and behavior. In: Bytnerowicz, A., Arbaugh, M.J., Riebau, A.R., Andersen, C. (Eds.), Wildland Fires and Air Pollution, Developments in Environmental Science. Elsevier, pp. 37–59. https://doi.org/10.1016/S1474-8177(08)00002-8.

Camiá, A., Amatulli, G., 2009. Weather factors and fire danger in the Mediterranean. In: Chuvieco, E. (Ed.), Earth Observation of Wildland Fires in Mediterranean Ecosystems. Springer-Verlag, pp. 71–82.

Cardil, A., Molina, D.M., Ramirez, J., Vega-García, C., 2013. Trends in adverse weather patterns and large wildland fires in Aragón (NE Spain) from 1978 to 2010. Nat. Hazards Earth Syst. Sci. 13, 1393–1399. https://doi.org/10.5194/nhess-13-1393-2013.

Cardil, A., Molina, D.M., Kobziar, L.N., 2014. Extreme temperature days and their potential impacts on southern Europe. Nat. Hazards Earth Syst. Sci. 14, 3005–3014. https://doi.org/10.5194/nhess-14-3005-2014.

Charrad, M., Ghazzali, N., Boiteau, V., Niknafs, A., 2014. {NbClust}: an {R} package for determining the relevant number of clusters in a data set. J. Stat. Softw. 61, 1–36.

Collaud Coen, M., Weingartner, E., Furger, M., Nyeki, S., Prévôt, A.S.H., Steinbacher, M., Baltensperger, U., 2011. Aerosol climatology and planetary boundary influence at the Jungfraujoch analyzed by synoptic weather types. Atmos. Chem. Phys. 11, 5931–5944. https://doi.org/10.5194/acp-11-5931-2011.

Cortesi, N., Gonzalez-Hidalgo, J.C., Trigo, R.M., Ramos, A.M., 2014. Weather types and spatial variability of precipitation in the Iberian Peninsula. Int. J. Climatol. 34, 2661–2677. https://doi.org/10.1002/joc.3866.

Duane, A., Brotons, L., 2018. Synoptic weather conditions and changing fire regimes in a Mediterranean environment. Agric. For. Meteorol. 253-254, 190–202. https://doi.org/10.1016/j.agrformet.2018.02.014.

Dunn, O.J., 1964. Multiple comparisons using rank sums. Technometrics 6, 241–252.

Fernández-González, S., del Río, S., Castro, A., Penas, A., Fernández-Raga, M., Calvo, A.I., Fraile, R., 2012. Connection between NAO, weather types and precipitation in León, Spain (1948–2008). Int. J. Climatol. 32, 2181–2196. https://doi.org/10.1002/joc.2431.

Fernández-Raga, M., Fraile, R., Keizer, J.J., Teijeiro, M.E.V., Castro, A., Palencia, C., Calvo, A.I., Koenders, J., Marques, R.L.D.C., 2010. The kinetic energy of rain measured with an optical disdrometer: an application to splash erosion. Atmos. Res. 96, 225–240. https://doi.org/10.1016/j.atmosres.2009.07.013.

Foster, L.I.D., Lees, A.J., 1999. Changing headwater suspended sediment yields in the LOIS catchments over the last century: a paleolimnological approach. Hydrol. Process. 13, 1137–1153. https://doi.org/10.1002/(SICI)1099-1085(199905)13:7<1137::AID-HYP794>3.0.CO;2-M.

Hidalgo-Muñoz, J.M., Argüeso, D., Gámiz-Fortis, S.R., Esteban-Parra, M.J., Castro-Díez, Y., 2011. Trends of extreme precipitation and associated synoptic patterns over the southern Iberian Peninsula. J. Hydrol. 409, 497–511. https://doi.org/10.1016/j.jhydrol.2011.08.049.

Holsinger, L., Parks, S.A., Miller, C., 2016. Weather, fuels, and topography impede wildland fire spread in western US landscapes. For. Ecol. Manag. 380, 59–69. https://doi.org/10.1016/j.foreco.2016.08.035.

Jiménez-Ruano, A., Rodrigues Mimbrero, M., de la, Riva, Fernández, J., 2017. Exploring spatial–temporal dynamics of fire regime features in mainland Spain. Nat. Hazards Earth Syst. Sci. 17, 1697–1711. https://doi.org/10.5194/nhess-17-1697-2017.

Koutsias, N., Arianoutsou, M., Kallimanis, A.S., Mallinis, G., Halley, J.M., Dimopoulos, P., 2012. Where did the fires burn in Peloponnisos, Greece the summer of 2007? Evidence for a synergy of fuel and weather. Agric. For. Meteorol. 156, 41–53. https://doi.org/10.1016/J.AGRFORMET.2011.12.006.

Koutsias, N., Allgöwer, B., Kalabokidis, K., Mallinis, G., Balatsos, P., Goldammer, J., 2016. Fire occurrence zoning from local to global scale in the European Mediterranean basin: implications for multi-scale fire management and policy. IForest 9, 195–204.

Krebs, P., Pezzatti, G.B., Mazzoleni, S., Talbot, L.M., Conedera, M., 2010. Fire regime: history and definition of a key concept in disturbance ecology. Theory Biosci. 129, 53–69. https://doi.org/10.1007/s12064-010-0082-z.

Kruskal, W.H., Wallis, A., 1952. Use of ranks in one-criterion variance analysis. J. Am. Stat. Assoc. 47, 583–621.

Leone, V., Koutsias, N., Martínez, J., Vega-García, C., Allgöwer, B., Lovreglio, R., 2003. The human factor in fire danger assessment. In: Chuvieco, E. (Ed.), Wildland Fire Danger Estimation and Mapping. The Role of Remote Sensing Data. World Scientific Publishing, Singapore.

Liao, Z., Gao, M., Sun, J., Fan, S., 2017. The impact of synoptic circulation on air quality and pollution-related human health in the Yangtze River Delta region. Sci. Total Environ. 607–608, 838–846. https://doi.org/10.1016/j.scitotenv.2017.07.031.

Liu, Z., Wimberly, M.C., 2015. Climatic and landscape influences on fire regimes from 1984 to 2010 in the Western United States. PLoS One 10, e0140839. https://doi.org/10.1371/journal.pone.0140839.

Liu, Z., Yang, J., Chang, Y., Weisberg, P.J., He, H.S., 2012. Spatial patterns and drivers of fire occurrence and its future trend under climate change in a boreal forest of northeast China. Glob. Change Biol. 18, 2041–2056. https://doi.org/10.1111/j.1365-2486.2012.02649.x.

MAPAMA, 2012. Los Incendios Forestales en España. Decenio 2001-2010. Madrid. .

Martínez, J., Vega-Garcia, C., Chuvieco, E., 2009. Human-caused wildfire risk rating for prevention planning in Spain. J. Environ. Manag. 90, 1241–1252. https://doi.org/10.1016/j.jenvman.2008.07.005.

Martín-Vide, J., Olcina, J., 2001. Climas y tiempos de España. Alianza editorial, Madrid. .

Messeri, A., Morabito, M., Messeri, G., Brandani, G., Petralli, M., Natali, F., Grifoni, D., Crisci, A., Gensini, G., Orlandini, S., 2016. Weather-related flood and landslide damage: a risk index for Italian regions. PLoS One 10, 1–17. https://doi.org/10.1371/journal.pone.0144468.

Meyn, A., White, P.S., Buhk, C., Jentsch, A., 2007. Environmental drivers of large, infrequent wildfires: the emerging conceptual model. Prog. Phys. Geogr. 31, 287–312. https://doi.org/10.1177/0309133307079365.

Montserrat, D., 2000. Mapas sinópticos medios correspondientes al inicio de grandes incendios forestales en Catalunya. AEC, Publicaciones La Asoc, Española Climatol, pp. 339–346 Ser. A 1.

Moreno, M.V., Conedera, M., Chuvieco, E., Pezzatti, G.B., 2014. Fire regime changes and major driving forces in Spain from 1968 to 2010. Environ. Sci. Policy 37, 11–22. https://doi.org/10.1016/j.envsci.2013.08.005.

Nadal-Romero, E., González-Hidalgo, J.C., Cortesi, N., Desir, G., Gómez, J.A., Lasanta, T., Lucía, A., Marín, C., Martínez-Murillo, J.F., Pacheco, E., Rodríguez-Blanco, M.L., Díaz, A., Ruiz-Sinoga, J.D., Taguas, E.V., Taboada-Castro, M.M., Taboada-Castro, M.T., Úbeda, X., Zabaleta, A., 2015. Relationship of runoff, erosion and sediment yield to weather types in the Iberian Peninsula. Geomorphology 228, 372–381. https://doi.org/10.1016/j.geomorph.2014.09.011.

Papadopoulos, A., PaschalidouEmail, A.K., Kassomenos, P.A., McGregor, G., 2013. On the association between synoptic circulation and wildfires in the Eastern Mediterranean. Theor. Appl. Climatol. 115, 483–501.

Parisien, M.-A., Moritz, M.A., 2009. Environmental controls on the distribution of wildfire at multiple spatial scales. Ecol. Monogr. 79, 127–154. https://doi.org/10.1890/07-1289.1.

Paschalidou, A.K., Kassomenos, P.A., 2016. What are the most fire-dangerous atmospheric circulations in the Eastern-Mediterranean? Analysis of the synoptic wildfire climatology. Sci. Total Environ. https://doi.org/10.1016/j.scitotenv.2015.09.039.

Peña-Angulo, D., Trigo, R.M., Cortesi, N., González-Hidalgo, J.C., 2016. The influence of weather types on the monthly average maximum and minimum temperatures in the Iberian Peninsula. Atmos. Res. 178–179, 217–230. https://doi.org/10.1016/J.ATMOSRES.2016.03.022.

Piñol, J., Terradas, J., Lloret, F., 1998. Climate warming, wildfire hazard, and wildfire occurrence in Coastal Eastern Spain. Clim. Change 38, 345–357. https://doi.org/10.1023/A:1005316632105.

R Core Team, R Development Team Core, 2017. R: A Language and Environment for Statistical Computing.

Rodrigues, M., Jiménez, A., de la Riva, J., 2016. Analysis of recent spatial–temporal evolution of human driving factors of wildfires in Spain. Nat. Hazards. https://doi.org/10.1007/s11069-016-2533-4.

Rodrigues, M., Jiménez-Ruano, A., Peña-Angulo, D., de la Riva, J., 2018. A comprehensive spatial-temporal analysis of driving factors of human-caused wildfires in Spain using geographically weighted logistic regression. J. Environ. Manag. 225, 177–192. https://doi.org/10.1016/j.jenvman.2018.07.098.

Royé, D., Taboada, J.J., Martí, A., Lorenzo, M.N., 2016. Winter circulation weather types and hospital admissions for respiratory diseases in Galicia, Spain. Int. J. Biometeorol. 60, 507–520. https://doi.org/10.1007/s00484-015-1047-1.

Ruffault, J., Curt, T., Martin St-Paul, N.K., Moron, V., Trigo, R.M., 2017a. Extreme wildfire occurrence in response to global change type droughts in the Northern Mediterranean. Nat. Hazards Earth Syst. Sci. Discuss. 2017, 1–21. https://doi.org/10.5194/nhess-2017-415.

Ruffault, J., Moron, V., Trigo, R.M., Curt, T., 2017b. Daily synoptic conditions associated

with large fire occurrence in Mediterranean France: evidence for a wind-driven fire regime. Int. J. Climatol. 37, 524–533. https://doi.org/10.1002/joc.4680.
Russo, A., Gouveia, C.M., Páscoa, P., DaCamara, C.C., Sousa, P.M., Trigo, R.M., 2017. Assessing the role of drought events on wildfires in the Iberian Peninsula. Agric. For. Meteorol. 237–238, 50–59. https://doi.org/10.1016/j.agrformet.2017.01.021.
Salis, M., Arca, B., Alcasena, F., Arianoutsou, M., Bacciu, V., Duce, P., Duguy, B., Koutsias, N., Mallinis, G., Mitsopoulos, I., Moreno, J.M., Pérez, J.R., Urbieta, I.R., Xystrakis, F., Zavala, G., Spano, D., 2016. Predicting wildfire spread and behaviour in Mediterranean landscapes. Int. J. Wildl. Fire 25, 1015–1032.
San-Miguel Ayanz, J., Camia, A., 2009. Forest fires at a glance: facts, figures and trends in the EU. In: Birot, Y. (Ed.), Living with Wildfires: What Science Can Tell Us. A Contribution to the Science-Policy Dialogue. European Forest Institute, pp. 11–18.
San-Miguel-Ayanz, J., Schulte, E., Schmuck, G., Camia, A., 2013. The European Forest fire information system in the context of environmental policies of the European Union. For. Policy Econ. 29, 19–25. https://doi.org/10.1016/j.forpol.2011.08.012.
Santurtún, A., González-Hidalgo, J.C., Sanchez-Lorenzo, A., Zarrabeitia, M.T., 2015. Surface ozone concentration trends and its relationship with weather types in Spain (2001–2010). Atmos. Environ. 101, 10–22. https://doi.org/10.1016/j.atmosenv.2014.11.005.
Sorensen, T.J., 1948. A Method of Establishing Groups of Equal Amplitude in Plant Sociology Based on Similarity of Species Content and Its Application to Analyses of the Vegetation on Danish Commons. I kommission hos E. Munksgaard, Kobenhavn.
Teale, N.G., Quiring, S.M., Ford, T.W., 2017. Association of synoptic-scale atmospheric patterns with flash flooding in watersheds of the New York City water supply system. Int. J. Climatol. 37, 358–370. https://doi.org/10.1002/joc.4709.
Thompson, M., Calkin, D., Finney, M., Ager, A., Gilbertson-Day, J., 2011. Integrated national-scale assessment of wildfire risk to human and ecological values. Stoch. Environ. Res. Risk Assess. 25, 761–780. https://doi.org/10.1007/s00477-011-0461-0.
Trigo, R.M., DaCamara, C.C., 2000. Circulation weather types and their influence on the precipitation regime in Portugal. Int. J. Climatol. 20, 1559–1581. https://doi.org/10.1002/1097-0088(20001115)20:13<1559::AID-JOC555>3.0.CO;2-5.
Trigo, R.M., Sousa, P.M., Pereira, M.G., Rasilla, D., Gouveia, C.M., 2016. Modelling wildfire activity in Iberia with different atmospheric circulation weather types. Int. J. Climatol. 36, 2761–2778. https://doi.org/10.1002/joc.3749.
Turco, M., Llasat, M.C., von Hardenberg, J., Provenzale, A., 2013. Impact of climate variability on summer fires in a Mediterranean environment (northeastern Iberian Peninsula). Clim. Change 116, 665–678. https://doi.org/10.1007/s10584-012-0505-6.
Urbieta, I.R., Zavala, G., Bedia, J., Gutiérrez, J.M., Miguel-Ayanz, J.S., Camia, A., Keeley, J.E., Moreno, J.M., 2015. Fire activity as a function of fire–weather seasonal severity and antecedent climate across spatial scales in southern Europe and Pacific western USA. Environ. Res. Lett. 10, 114013. https://doi.org/10.1088/1748-9326/10/11/114013.
Wastl, C., Schunk, C., Lüpke, M., Cocca, G., Conedera, M., Valese, E., Menzel, A., 2013. Large-scale weather types, forest fire danger, and wildfire occurrence in the Alps. Agric. For. Meteorol. 168, 15–25. https://doi.org/10.1016/J.AGRFORMET.2012.08.011.
Wheater, C.P., Cook, P.A., 2000. Using Statistics to Understand the Environment, 1st ed. Routledge, London and New York.
Wilby, R.L., Dalgleish, H.Y., Foster, I.D.L., 1998. The impact of weather patterns on historic and contemporary catchment sediment yields. Earth Surf. Process. Landforms 22, 353–363. https://doi.org/10.1002/(SICI)1096-9837(199704)22:4<353::AID-ESP692>3.0.CO;2-G.